A R C H I V E S O F M E T A L L U R G Y A N D M A T E R I A L S
Volume 56 2011 Issue 3
DOI: 10.2478/v10172-011-0061-5

K. WIERZBANOWSKI*, M. WROŃSKI*, A. BACZMAŃSKI*, B. BACROIX**, P. LIPINSKI*** , A. LODINI****

PROBLEM OF LATTICE ROTATION DUE TO PLASTIC DEFORMATION. EXAMPLE OF ROLLING OF F.C.C MATERIALS

PROBLEM OBROTU SIECI KRYSTALICZNEJ PODCZAS ODKSZTAŁCENIA PLASTYCZNEGO. PRZYKŁAD WALCOWANIA MATERIAŁÓW O SIECI REGULARNEJ PŁASKO CENTROWANEJ

Rotations of grain crystal lattice are responsible for texture formation during plastic deformation. The classical definition of lattice rotation leads in some cases to different texture predictions than the definition based on the orientation preservation of selected sample directions and/or planes. For example, if classical <110>{111} slip is taken into account for f.c.c. materials, the former approach enables to predict both copper and brass types of rolling texture, while classical approach predicts only the first one. The analysis of rolling process was done for two types of lattice rotation and in function of grain-matrix interaction parameter used in a deformation model. Correlation factors estimating the similarity of predicted and experimental textures as well as the shares of ideal orientations are discussed.

Keywords: lattice rotation, elasto-plastic deformation models, copper-brass texture transition, rolling deformation

Obroty sieci krystalograficznej ziaren są odpowiedzialne za powstania tekstury podczas odkształcenia plastycznego. Klasyczna definicja obrotu sieci prowadzi w pewnych przypadkach do innych przewidywań tekstury niż definicja oparta na warunku zachowania wybranych kierunków lub płaszczyzn próbki. Na przykład biorąc pod uwagę systemy poślizgu <110>{111}, użycie tej drugiej pozwala przewidzieć zarówno teksturę typu miedzi jak i mosiądzu, podczas gdy definicja klasyczna umożliwia przewidywanie jedynie tekstury typu miedzi. Dokonano analizy odkształcenia przez walcowanie dla obu definicji obrotu uwzględniając równocześnie wpływ parametru oddziaływania ziarna z otaczającym materiałem. W celu porównania przewidzianych i zmierzonych tekstur wyliczono i przedyskutowano współczynniki korelacji oraz udziały orientacji idealnych.

1. Introduction

Modelling of polycrystalline plastic deformation is an important field of the material science. It enables to study deformation mechanisms, microstructure modification and orientation distributions. A comparison of predicted and experimental deformation texture is one of the most important tests confirming, whether a model is correctly constructed. Texture predictions allow also to plan optimal deformation processes in order to obtain required material properties.

Obviously, predicted textures depend on the applied definition of lattice rotation. In many works the *classical* (CL) definition is used and it is based on the assumption that a rigid body rotation of each grain and of the sample are the same, at least statistically (in rolling deformation they are equal to zero) [1-4]). Consequently, the lattice rotation is calculated in order to fulfil this condition.

The other approach is based on the assumption that selected sample and grain planes and/or directions preserve constant orientation with respect to the laboratory reference frame (the latter is defined by the deformation geometry). This approach, named by the present authors *preservation* (PR) condition, was successfully used in modelling of plane strain or axially symmetric deformation (e.g., [5-8]). In general, a characteristic microstructure produced during deformation (e.g., elongation and flattening of grains during rolling) explains a use of PR definition [2]. It should be mentioned that also other lattice rotation definitions are used in different versions of the self consistent model (e.g., [9-13]).

For clarity, we compare only CL and PR lattice rotation definitions in this work. They can be implemented

* AGH UNIVERSITY OF SCIENCE AND TECHNOLOGY, FACULTY OF PHYSICS AND APPLIED COMPUTER SCIENCE, 30-059 KRAKÓW, 30 MICKIEWICZA AV., POLAND
** LSPM - CNRS, UNIVERSITÉ PARIS 13, 99 AV. J.B. CLÉMENT, 93430 VILLETANEUSE, FRANCE
*** LABPS, ECOLE NATIONALE D'INGENIEURS DE METZ, ILE DU SAULCY, 57045 METZ, FRANCE
**** LACM-DTI, UNIVERSITÉ DE REIMS CHAMPAGNE ARDENNE, 9, BD. DE LA PAIX, 51100 REIMS, FRANCE

in any elasto-plastic deformation model. We use a deformation model [4], which is shortly characterized in the next Section. Besides the lattice rotation also the intensity of grain-matrix interaction has a strong influence on the predicted results (e.g., crystallographic textures). Hence, this factor will be also taken into account in considerations.

2. Deformation model used in calculations

Lets us shortly review basic variables used in applied deformation model.

2.1. Grain-matrix interactions

The main question, which has to be answered in any deformation model, is: what is a relation between macroscopic variables of the sample (stress Σ_{ij} and deformation E_{ij}) and analogous ones (σ_{ij}, ε_{ij}) appearing on grain level – Fig. 1. Unfortunately, it is not possible to solve this problem in a general case. It is the reason why we use models.

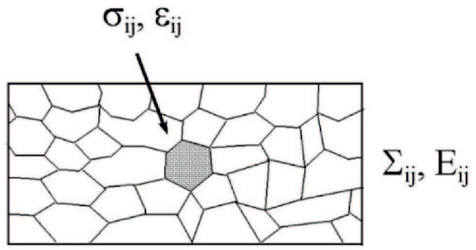

Fig. 1. Macroscopic load Σ_{ij} is applied to a material, while a local stress σ_{ij} appears on a grain level. The sample deformation is E_{ij} and a grain deformation is ε_{ij}

It was shown by Hill [14] that a general relation between local and global variables can be written in the form:

$$\dot{\sigma}_{ij} = \dot{\Sigma}_{ij} + L_{ijkl}(\dot{E}_{kl} - \dot{\varepsilon}_{kl}) \qquad (1)$$

where $\dot{\sigma}_{ij}$, $\dot{\varepsilon}_{ij}$ are local stress and strain rates, $\dot{\Sigma}_{ij}$, $\dot{E}_{ij}$ their global equivalents, L_{ijkl} is the interaction tensor and the convention of summation on the repeated index is applied (it is used in all formula in this paper).

A strict calculation of L_{ijkl} tensor is impossible in a general case; hence some assumptions have to be used leading to various, more or less accurate, models. A considerable progress was employing the self consistent method to such problems [9-13]. Nevertheless, in many cases the assumption of isotropic matrix-grain interaction leads to surprisingly good predictions of material properties. In such the case L_{ijkl} tensor can be replaced by a scalar parameter. Moreover, in the cases of practical importance, it can be assumed that the plastic strain rate term ($\dot{E}^p_{ij} - \dot{\varepsilon}^p_{ij}$) is much larger than the elastic one ($\dot{E}^e_{ij} - \dot{\varepsilon}^e_{ij}$). Accordingly, and under additive strain rate decomposition approximation, Eq. 1 can be simplified to the following form [3,4]:

$$\dot{\sigma}_{ij} = \dot{\Sigma}_{ij} + \alpha G\,(\dot{E}^p_{ij} - \dot{\varepsilon}^p_{ij}) \qquad (2)$$

where G is the shear modulus of the material and α is so called elasto-plastic accommodation parameter. Eq. 2 states that the rate of local stress σ_{ij} is a superposition of the rate of applied external stress Σ_{ij} and the rate of interaction term:α $G\,(E^p_{ij} - \varepsilon^p_{ij})$. The latter term can be called *reaction stress* and is responsible for a deformed grain shape: it tends to minimize the difference between a grain shape and the sample shape (analogous, but simpler relation was used in original Leffers model [6]). Some of known models can be deduced from Eq. 2 if α takes appropriate values. For example, α=0 leads to the Sachs model [15] ($\sigma_{ij} = \Sigma_{ij}$). Taking $\alpha \to \infty$ one approaches the Taylor model [16] ($\varepsilon^p_{ij} = E^p_{ij}$). On the other hand, α=1 leads to Kröner scheme [17], in which a purely elastic interaction between a grain and the matrix is assumed. However, it was shown, that a magnitude of interaction in polycrystalline metals is much weaker than a purely elastic one [3]. Hence, the realistic values of α, taken into account in our calculations, are between 0.001 and 0.1.

2.2. Description of deformation by slip

An exhaustive review of deformation mechanisms in polycrystalline materials can be found in the monograph [18]. Slip and twinning are two basic crystallographic mechanisms of plastic deformation. Twinning can appear in h.c.p. and in some f.c.c. metals, especially if they are deformed with high strain rates or at low temperatures. However, in f.c.c. metals deformed at room temperature, crystallographic slip is the dominating mechanism. Consequently, only slip is taken into account in the present calculations.

During slip two parts of a crystal are irreversibly sheared one with respect to other by a multiple of interatomic distance (Fig. 2). The shearing movement occurs on a crystallographic slip plane (hkl) (characterized by **n** normal unit vector) and along a slip direction vector [uvw] (characterized by **m** unit vector). Consequently one defines [uvw](hkl) slip system, which also can be shortly denoted as (**m**, **n**). The crystallographic slip mechanism is schematically presented in Fig. 3b, where also the slip shear strain γ is defined. By activation of at least five independent slip systems one can produce any imposed plastic strain.

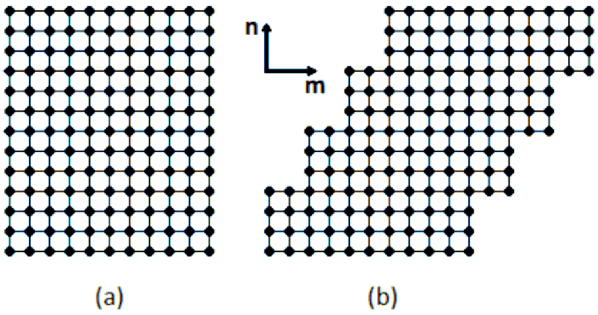

Fig. 2. Deformation by crystallographic slip a) crystal before slip, b) blocs of crystal are sheared on the slip plane (**n**) along the slip direction (**m**)

It is useful to introduce the reference frame connected with the slip system: $\boldsymbol{x}_1^g$ =**m** and $\boldsymbol{x}_3^g$ = **n** (Fig. 3a). The resolved shear stress, decisive for a slip system activation, is easily expressed in this coordinates system: $\tau = \sigma_{13}^g$. In a similar way, the glide shear $d\gamma$ of a single slip produces only one non-zero component of the plastic displacement gradient: $d\gamma = de_{13}^{p\ (g)}$.

The condition for slip occurrence is:

$$\tau = \tau_{cr} \tag{3}$$

i.e., the resolved shear stress ($\tau = \sigma_{13}^g$) has to reach the critical valueτ_{cr} (Schmid law).

If Cauchy stress definition is used, the resolved shear stress $\tau = \sigma_{13}^g$ on the slip system (**m**, **n**) is expressed as:

$$\tau = \sigma_{13}^g = m_i n_j \sigma_{ij} \tag{4}$$

where σ_{ij} (grain stress), **m** and **n** vectors are expressed in the laboratory reference frame {L}. In the case of rolling, the {L} frame is defined as follows: x_1 is parallel to rolling direction, x_2 – to transverse direction and x_3 – to normal direction.

Slip systems are hardened during deformation, which is visible in the stress-strain curve. The physical reason of hardening is mutual interaction of dislocations, which are intensively multiplied during deformation. Dislocations are necessary for a progress of plastic strain, but being in a huge amount they also block each other. This increases the critical shear stress for slip. Generally, a multi-slip is developed; hence a hardening of the slip system ("*i*") depends on shear glides on other active slip systems ("*j*"):

$$d\tau_{cr}^i = H^{ij} d\gamma^j \tag{5}$$

where H^{ij} is the strain hardening matrix. Both theoretical and experimental studies show that in the first approximation this matrix contains two types of terms: strong (h_2) and weak ones (h_1) [19]. However, in the present calculations we used the isotropic hardening matrix, i.e., h_1=h_2.

2.3. Grain and sample deformation

Let us consider a typical increment of external load. First, let us express the strain, resulting from a glide on *one* slip system with a very small shear amplitude $\delta\gamma$. In the slip system reference frame (***g***) the plastic displacement gradient tensor has only one non-zero component: $\delta e_{13}^{p(g)} = \delta\gamma$. This tensor after transformation to the laboratory reference frame {L} is:

$$\delta e_{ij}^p = m_i n_j \, \delta e_{13}^{p(g)} = m_i n_j \delta\gamma \tag{6}$$

The plastic strain increment, $\delta\varepsilon_{ij}^p$, is the symmetric part of δe_{ij}^p:

$$\delta\varepsilon_{ij}^p = \frac{1}{2}(m_i n_j + m_j n_i)\,\delta\gamma \tag{7}$$

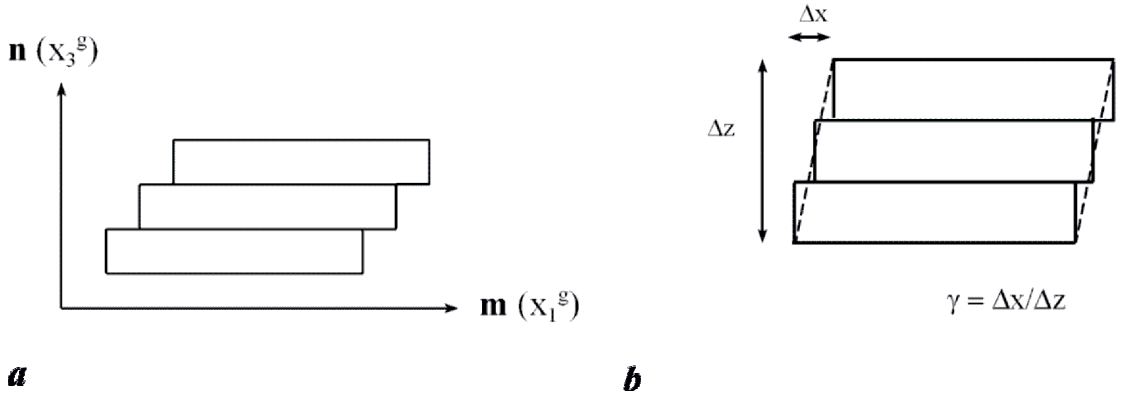

Fig. 3. a) Reference frame (**g**) connected to a single slip system: x_1^g is defined by **m** vector and x_3^g – by **n** vector, b) definition of the glide shear γ on a single slip system

After each elementary slip event, all basic quantities are recalculated (crystal orientation, reaction stress, sample deformation). A total plastic strain increment of grain "*I*", developed during the considered external load increment, is the sum of consecutive glides on the most loaded slip systems (*s*), each with a fixed and small shear magnitude ($\delta\gamma^s = \delta\gamma$ in our case):

$$\Delta\varepsilon_{ij}^{p(I)} = \sum_s \left[\frac{1}{2}(m_i^s n_j^s + m_j^s n_i^s)\,\delta\gamma^s\right] \tag{8}$$

The number of elementary slip events depends on the local stress according to Eq. 2. The corresponding overall plastic strain increment is the average of grain strains:

$$\Delta E_{ij}^p =< \Delta\varepsilon_{ij}^{p(I)} >= \frac{1}{V_0}\Delta\varepsilon_{ij}^{p(I)} V^I \tag{9}$$

where V^I and V_0 are the volumes of the I-th grain and the sample, respectively.

3. Crystal lattice rotation

Let us consider for simplicity a crystallite in a form of the square plate ABCD (we deal with a quasi 2-D situation), with its edges parallel to the axes of the laboratory coordinates frame {L}, see Fig. 4. The grain is then deformed by a homogenous shear $\delta\gamma$ on the slip system (**n, m**) into configuration A'B'C'D'. The resultant grain shape *after one slip event*, shown in Fig. 4b, is characterized by the plastic strain (Eq. 7) and by the rigid body rotation (plastic rotation):

$$\delta\omega_{ij}^p = \frac{1}{2}(\delta e_{ij}^p - \delta\, e_{ij}^p) = \frac{1}{2}(m_i n_j - m_j n_i)\;\delta\gamma \tag{10}$$

If there was no interaction between a grain and its surrounding – the *crystal lattice* orientation would not change even for not zero $\delta\omega_{ij}^p$ (Fig. 4 a,b). However, some constraints are always imposed on the deformed grain by a neighbouring material and by a deformation device. As a consequence the crystal lattice will rotate from its initial position.

Let us consider such a deformation process, that the total sample rotation is zero ($\delta\Omega_{ij} = 0$); this is, e.g., the case of rolling or of tensile test. Next, let us do the approximation, that the total rotations of a grain and of the sample are the same, i.e.: $\delta\omega_{ij} = \delta\Omega_{ij} = 0$. To fulfil this condition, a compensating rotation of a grain $\delta\omega_{ij}^{latt(CL)}$ (classical lattice rotation – CL) has to be added the plastic rotation:

$$\delta\omega_{ij} = \delta\omega_{ij}^p + \delta\omega_{ij}^{latt(CL)} = 0 \tag{11}$$

Finally, from Eqs. 10 and 11 we obtain:

$$\delta\omega_{ij}^{latt(CL)} = -\delta\omega_{ij}^p = -\frac{1}{2}(m_i n_j - m_j n_i)\;\delta\gamma \tag{12}$$

The above equation gives the definition of classical lattice rotation (CL).

In our example from Fig. 4 the lattice rotation component $\delta\omega_{31}^{latt(CL)} = -\frac{1}{2}(m_3 n_1 - m_1 n_3)\delta\gamma$ is imposed and it leads to the final position of the grain shown in Fig. 4c. It is visible, that the lattice orientation changed after this rotation.

However, it was found by some authors (e.g., [1,2], [5-8], [20]) that another approach to lattice rotation can be considered. In this approach the lattice rotation results from constraints limiting possible reorientations of specified sample directions and/or planes with respect to the laboratory reference frame {L}. Consequently, some restrictions are imposed on *selected* shear components *kl* (*where k≠l*) of the displacement gradient tensor, expressed in {L}, for the sample ($\delta G_{kl}^{)}$ and for a grain (δe_{kl}). If the grain shapes follow statistically that of the sample, one can assume (in the first approximation) that these selected components (*kl*) are the same for the sample and for a grain: $\delta G_{kl} = \delta e_{kl}$ [20]. For very strong constraints (e.g., case of rolling), the orientations of specified sample directions/planes are constant in {L} reference frame, hence: $\delta G_{kl} = \delta e_{kl} = 0$. Consequently, an auxiliary rotation (lattice rotation), has to be imposed on a grain in order to fulfil this condition:

$$\delta e_{kl} = \delta e_{kl}^p + \delta\omega_{kl}^{latt(PR)} = 0 \tag{13}$$

Or, substituting Eq.6:

$$\delta\omega_{kl}^{latt(PR)} = -\delta e_{kl}^p = -m_k n_l\,\delta\gamma \tag{14}$$

The above equation describes the *preservation condition* (PR) definition.

Let us return to our example from Fig. 4 and let us assume that the orientation of a string of material parallel to x_1 axis has to be constant. Consequently, $\delta\omega_{31}^{latt(PC)} = -m_3 n_1\,\delta\gamma$ rotation component has to be imposed. It changes the lattice rotation. The grain position after occurrence of this rotation is shown in Fig. 4d. It is visible that CL and PR lattice rotations are different (compare Figs. 4c and 4d).

Finally, let us calculate (following example from [2]) the difference between CL and PR lattice rotations (defined by Eqs. 12 and 13). For example: $\Delta\delta\omega_{31}^{latt} =$

$$\delta\omega_{31}^{latt(CL)} - \delta\omega_{31}^{latt(PR)} = -\tfrac{1}{2}(m_3 n_1 - m_1 n_3)\,\delta\gamma + \\ + m_3 n_1\delta\gamma = \tfrac{1}{2}(m_3 n_1 + m_1 n_3)\;\delta\gamma = \delta\varepsilon_{31}$$

This result is directly seen in Figs 4 c and d.

Analogous relations are fulfilled for other components:

$$\Delta\delta\omega_{21}^{latt} = \delta\varepsilon_{21}, \quad \Delta\delta\omega_{31}^{latt} = \delta\varepsilon_{31}, \quad \Delta\delta\omega_{32}^{latt} = \delta\varepsilon_{32} \tag{15}$$

It is clear that in the case where $\delta\varepsilon_{32} = \delta\varepsilon_{32} = \delta\varepsilon_{32} = 0$, both definitions lead to the same lattice rotations.

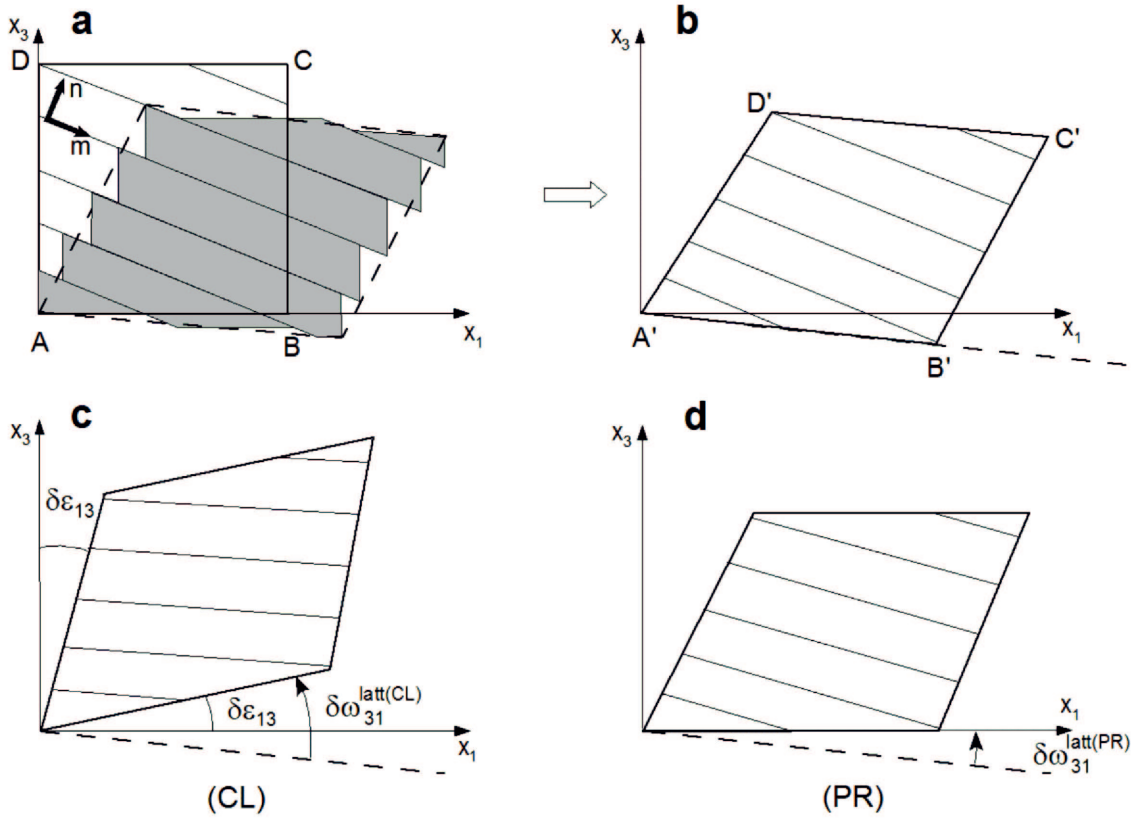

Fig. 4. a) Shear deformation of an initial grain in a form of square plate ABCD (with edges parallel to the laboratory reference frame {L}); the shear occurred on the slip system (**n**, **m**), b) shape and position of the grain (A'B'C'D') after slip only, c) position of the grain after slip and CL lattice rotation, d) position of the grain after slip and PR lattice rotation (with the condition of constant orientation of a string of material parallel to x_1 direction)

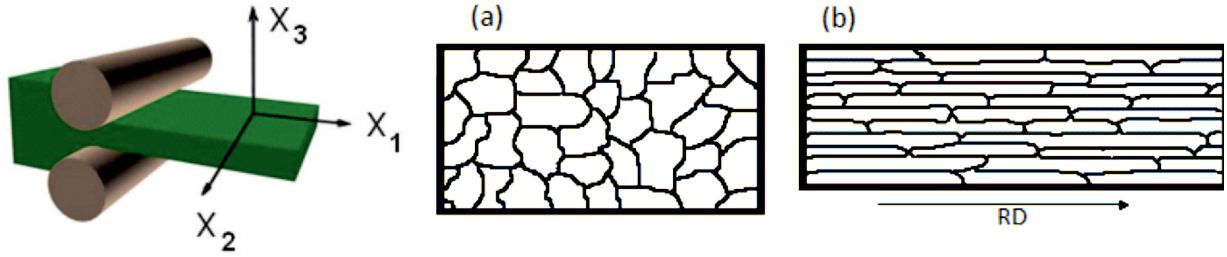

Fig. 5. Geometry of deformation by rolling. Grains shapes before (a) and after rolling (b)

4. PR definition of lattice rotation for rolling geometry

Let us consider the geometry of deformation by rolling (Fig. 5). The laboratory reference frame {L} is defined by x_1 axis parallel to the rolling direction and x_3 axis parallel to the normal direction. During rolling process, grains being initially equiaxial, become flattened and elongated in the rolling direction, similarly like the rolled sample (Fig.5 a,b). Hence, a string of material being initially parallel to the rolling direction (x_1) – preserves its orientation in the laboratory reference frame (at least statistically). Similarly, a platelet of material being initially parallel to the rolling plane (x_1x_2) – preserves its orientation. Consequently, δe_{31}, δe_{21} and δe_{32} components of the displacement gradient tensor have to be compensated by the opposite lattice rotation:

$$\begin{aligned} \delta\omega_{21}^{latt(PR)} &= -\delta e_{21} = -m_2 n_1 \delta\gamma \\ \delta\omega_{31}^{latt(PR)} &= -\delta e_{31} = -m_3 n_1 \delta\gamma \\ \delta\omega_{32}^{latt(PR)} &= -\delta e_{32} = -m_3 n_2 \delta\gamma \end{aligned} \tag{16}$$

and obviously: $\delta\omega_{ij}^{latt(PR)} = -\delta\omega_{ji}^{latt(PR)}$.

5. F.c.c. rolling textures predicted with CL and PR lattice rotation definitions

It is known that deformation models differ by the intensity of grain-matrix interaction. In the present model the interaction level is characterized by α parameter. Our calculations and comparison with experimental data confirm that one should consider α values from the [0.001, 0.1] range. A very strong interaction model (tending towards Taylor model) is already obtained for α of the order of one and a weak interaction one (tending towards Sachs model) - for α close to zero. These are two limiting values. To have a complete set of data, we performed calculations for α values from the range [0.0001, 1], for two definitions of lattice rotation, i.e., for CL and PR ones. The predicted orientation distribution functions (ODF) are compared with experimental data in Fig. 6 (for CL) and in Fig. 7 (for PR), while their quantitative analysis are presented in Figs. 8 and 9.

To discuss the predicted textures, four ideal orientations of f.c.c. rolling textures are marked in Figs. 6 and 7:

- copper component C: ($\varphi_1 = 90°$, $\phi = 35°$, $\varphi_2 = 45°$),
- brass component B: ($\varphi_1 = 35°$, $\phi = 45°$, $\varphi_2 = 0°$),
- S component: ($\varphi_1 = 59°$, $\phi = 37°$, $\varphi_2 = 63°$),
- Goss component G: ($\varphi_1 = 0°$, $\phi = 45°$, $\varphi_2 = 0°$).

(Euler angles characterizing crystal orientations are defined according to Bunge convention [21]). It is well known that two characteristic f.c.c. rolling textures are distinguished, namely the brass and the copper type textures. The problem is to explain the appearance of the brass type texture. There were many attempts to elucidate the transition between these two type textures. Consequently, some additional mechanisms like twining, cross-slip, slip on non-octahedral systems, slip by partial dislocations and shear band formation were considered [22,23]. However, in many cases the mentioned mechanisms do not appear with sufficient intensity, hence a simpler explanation of this texture transition can be expected.

In this paper, the <110>{111} slip is considered as the unique deformation mechanism of f.c.c. metals. Hence, a type of lattice rotation (CL or PR) and the intensity of grain-matrix interaction (α) are the two main variables, which decide on a character of predicted textures. The other model parameters used in computer simulations are listed in Table 1.

The predicted ODFs for α=0.001, 0.01, 0.02, 0.1 and for CL and PR definitions, as well as the experimental rolling textures of α-brass and copper, are shown in Figs. 6 and 7. In order to estimate the agreement of predicted and experimental textures, the linear regression was used and correlation factors R were calculated. The application of this method to texture comparison was described in details in [24]. Values of R vary in the range [0, 1]: two functions have identical shape if R=1 and are totally different if R=0. Also, the shares of selected ideal orientations in computer predicted textures were determined. For a given ideal orientation g_A, its share is calculated as a proportion of these model crystallites (all of the same volume) for which their crystal orientations g_i are distant from g_A less than 12 deg (i.e.: $\omega(g_i, g_A) \leqslant 12^0$).

For each predicted ODF we calculated a correlation factor estimating a degree of its similarity with experimental ODFs of α-brass (R_B) and of copper (R_C). These values are marked in Figs. 6 and 7. The variations of R_C and R_B and of the shares of ideal orientations versus α are shown in Figs. 8 and 9. The basic range of α (between 0.001 and 0.1) is indicated as a grey zone in these figures.

We note that R_C is clearly higher than R_B in the whole range of α for CL definition (Fig. 8). We also observe that the copper component (C) is strongly dominant over the brass component (B) in this approach – Fig. 9. Hence, we conclude that in the frame of CL definition only the copper texture can be predicted, independently of α value.

Contrary to that, PR definition leads to a more complex behaviour. For $\alpha < 0.01$ we obtain a texture close to the brass type one: R_B is evidently higher than R_C (also B component is predominant over C one) – Figs. 8 and 9. However, for $\alpha > 0.01$ the predicted texture becomes closer to the copper type one with a clear predominance of C orientation over B one ($R_C > R_B$).

Let us note that for a strong interaction level (α=0.1), the predicted textures for CL and PR definitions are practically identical and very close to the copper type texture (compare Figs. 6-9 for α=0.1). This results from the relation: $\delta\varepsilon_{32} = \delta\varepsilon_{32} = \delta\varepsilon_{32} = 0$ (valid for a strong interaction model), because accordingly to Eq. 15 CL and PR rotations are the same.

Finally, we conclude that in order to predict a rolling texture close to the experimental brass texture, one has to use PR rotation definition and a weak interaction level (α between 0.001 and 0.01). On the other hand, in the frame of CL definition it is not possible to forecast the brass type texture for any value of the interaction parameter α, if <110>{111} slip is considered as the unique deformation mechanism.

The above differences in predicted textures can influent some physical properties, e.g., the residual stress interpretations or material behaviour during recrystallization [25-28].

TABLE 1

Parameters used in the deformation model for polycrystalline copper

Number of grains	Slip systems	Initial value of $\tau_c r$	Hardening matrix terms	Slip shear increment	Applied stress components	Final rolling reduction	Shear modulus
N=5000	< 110 >{111}	τ^0_{cr}= 100 MPa	$h_1 = h_2$ = 60 MPa	$\Delta\gamma$=0,05	$\Sigma_{11} = -\Sigma_{33}$, other equal to zero	r = 50%	G=46 GPa

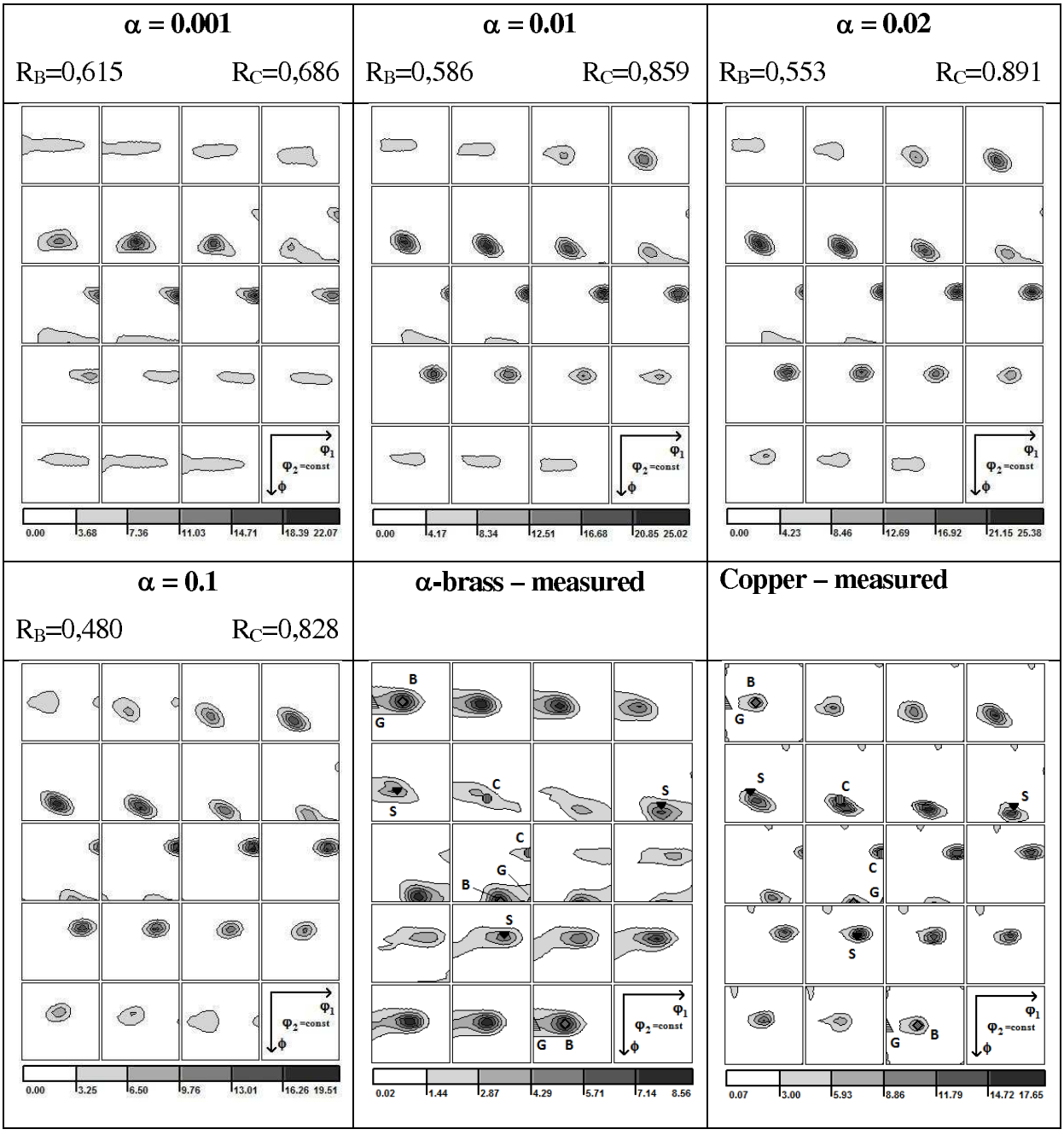

Fig. 6. Comparison of predicted rolling textures obtained for **CL** lattice rotation definition (50% rolling reduction) with experimental copper and α-brass textures. Results for α = 0.001, 0.01, 0.02 and 0.1 are shown

Ideal orientations are marked: C – {112} < $\bar{1}\bar{1}$1 >, B – {011} < 2$\bar{1}$1 >, S – {213} < $\bar{3}\bar{6}$4 > and G – {011} < 100 >

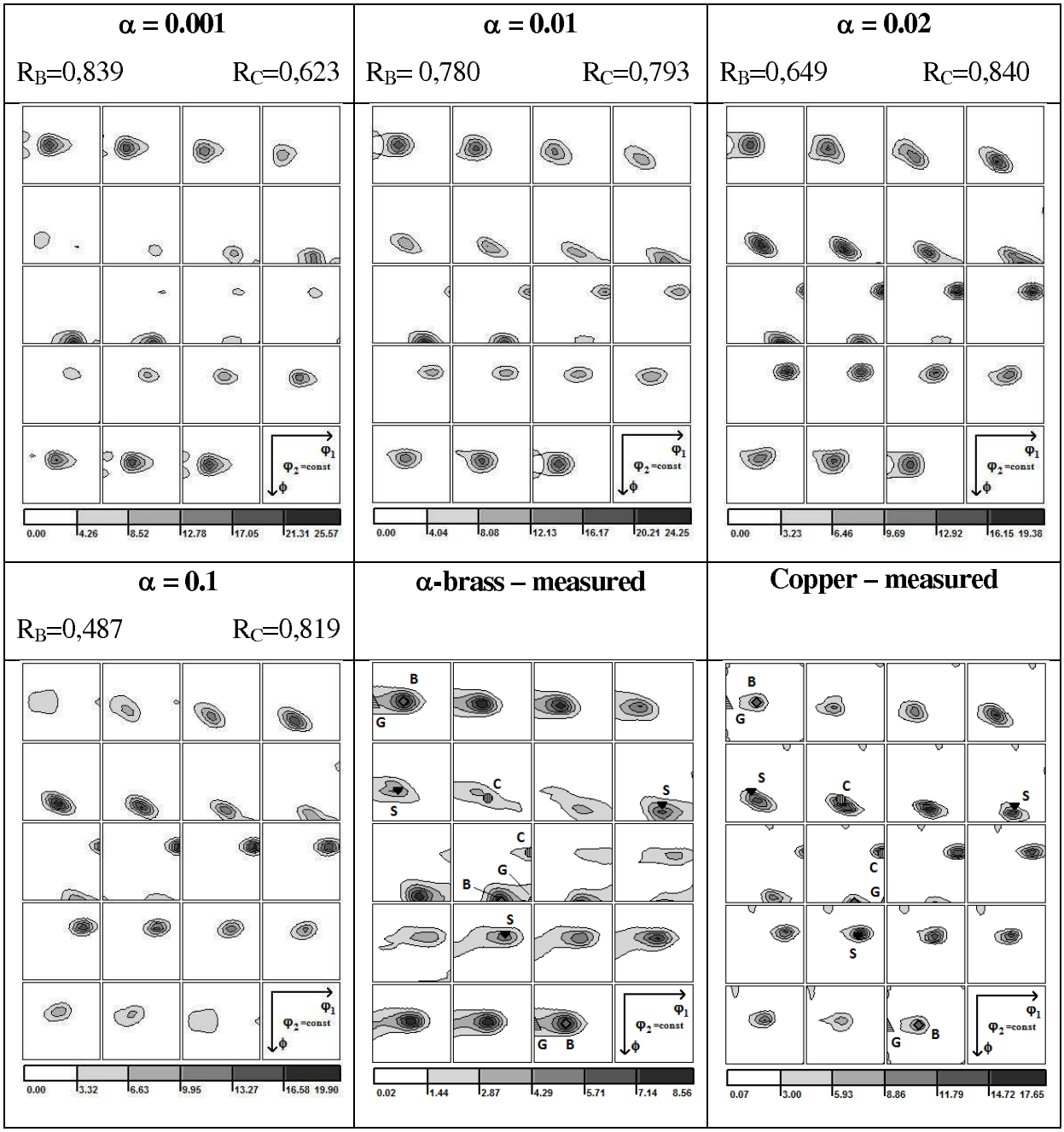

Fig. 7. Comparison of predicted rolling textures obtained for **PR** lattice rotation definition (50% rolling reduction) with experimental copper and α-brass textures. Results for α = 0.001, 0.01, 0.02 and 0.1 are shown

Ideal orientations are marked: C – {112} < $\bar{1}\bar{1}$1 >, B – {011} < 2$\bar{1}$1 >, S – {213} < $\bar{3}\bar{6}$4 > and G – {011} < 100 >

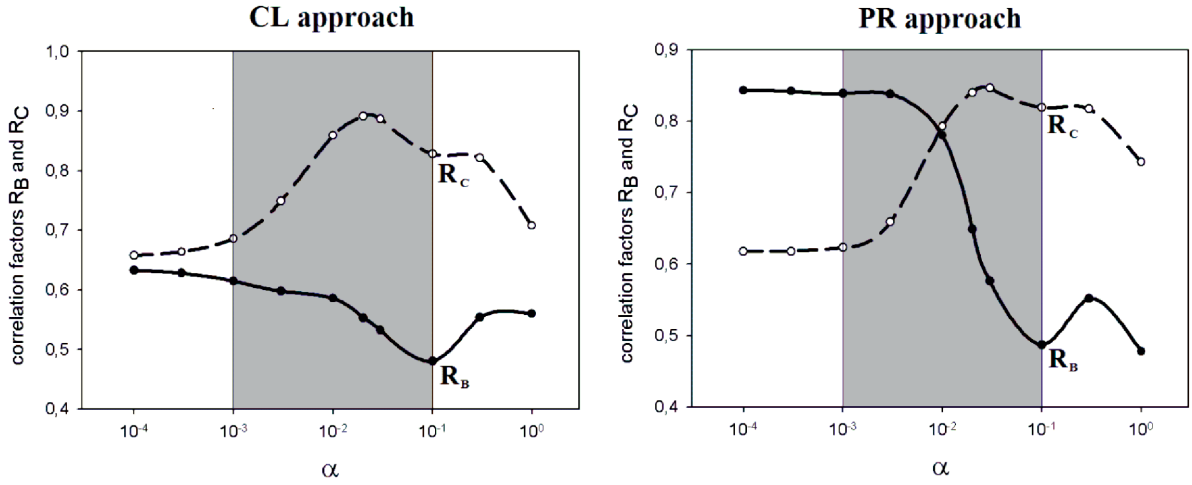

Fig. 8. Correlation factors R_B and R_C versus elasto-plastic accommodation parameter α. Results for CL and PR approaches are shown. Range of $\alpha \in [0.001, 0.1]$ is marked as grey zone

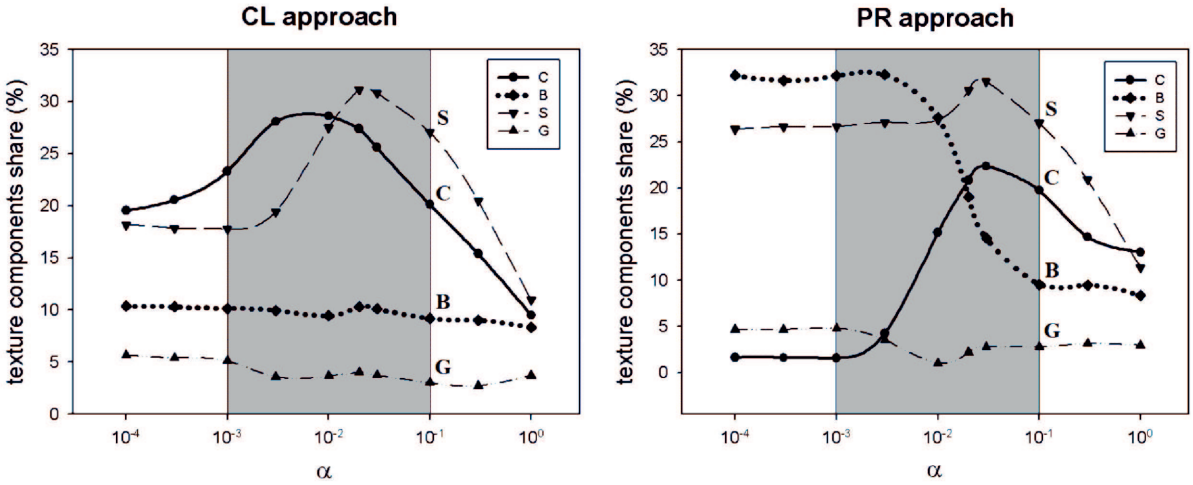

Fig. 9. Shares of four ideal orientations in predicted textures versus elasto-plastic accommodation parameter α. Results for CL and PR approaches are shown. Range of $\alpha \in [0.001, 0.1]$ is marked as grey zone

6. Conclusions

The presented calculations show that CL and PR definitions of lattice rotation lead in general to different rolling textures. The second important parameter is the elasto-plastic accommodation parameter α which describes the intensity of grain-matrix interaction.

The main conclusion is that for CL, independently of α value, it is not possible to predict the brass type texture, if the <110>{111} slip is the unique deformation mechanism; only the copper type texture can be obtained in this approach.

On the other hand, PR definition enables to predict both types of f.c.c rolling texture. For a weak interaction intensity (α between 0.001 and 0.01), one obtains the brass type texture, while for higher α values – the copper type texture. A continuous transition between two types of f.c.c rolling textures is observed in function of α parameter.

The above results confirm the importance of lattice rotation definition in deformation models. It has to be carefully chosen for a given geometry of deformation.

Acknowledgements

This work was supported by the Grants Nr: 712/N-POLONIUM/2010/0 and 3264/B/403/2011/40.

It was also supported by the Polish Ministry of Science and Higher Education (MNiSW).

REFERENCES

[1] W.F. Hosford, On Orientation Changes Accompanying Slip and Twinning, Texture of Crystalline Solids **2**, 175-182 (1977).

[2] T. Leffers, R.A. Lebensohn, Ambiguities in the calculation of lattice rotations for plane-strain deformation, Proc. of the 11th. Int. Conf. on Textures of Materials (ICOTOM-11), Z. Liang et al. eds., International Academic Publ., pp. 307-314 (1996).

[3] M. Berveiller, A. Zaoui, An Extension of the self-consistent scheme to plastically flowing polycrystals, J. Mech. Phys. Solids **26**, 325-344 (1979).

[4] K. Wierzbanowski, A. Baczmanski, P. Lipinski, A. Lodini, Elasto-plastic models of polycrystalline material deformation and their applications, Archives of Metallurgy and Materials **52,** 77-86 (2007).

[5] J. Tarasiuk, K. Wierzbanowski, J. Kuśnierz, Some Model Predictions for Plastically Deformed Polycrystalline Copper, Archives of Metallurgy **38**, 33-47 (1993).

[6] T. Leffers, Computer Simulation of the Plastic Deformation in Face-Centred Cubic polycrystals and the Rolling Texture Derived, phys. stat. sol. **25**, 337-344 (1968).

[7] K. Wierzbanowski, Numerical Prediction of Cross-Rolling and Compression Textures, Scripta Metallurgica **13**, 1117-1120 (1979).

[8] K. Wierzbanowski, J. Jura, W.G. Haije, R.B. Helmholdt, FCC Rolling Texture Transitions in Relation to Constraint Relaxation, Crystal Research and Technology **27**, 513-522 (1992).

[9] R.A. Lebensohn, T. Leffers, The Rules for the lattice rotation accompanying slip as derived from a self consistent model, Textures and Microstructures **31**, 217-230 (1999).

[10] S. Tiem, M. Berveiller, G.R. Canova, Grain shape effects on the slip system activity and on the lattice rotations, Acta Metall. **34**, 2134-2149 (1986).

[11] P. Lipinski, M. Berveiler, Elastoplasticity of micro-inhomogeneous metals at large strains, Int. Journal of Plasticity **5**, 149-172 (1989).

[12] R.A. Lebensohn, C.N. Tome, A selfconsistent approach for the simulation of plastic deformation and texture development of polycrystals: application to Zirconium alloys, Acta Metall. et Mater. **41**, 2611-2624 (1993).

[13] A. Molinari, G.R. Canova, S. Ahzi, A self consistent approach of the large deformation polycrystal viscoplasticity, Acta Metall. **35**, 2983-2994 (1987).

[14] R. Hill, Continuum Micro-Mechanics of Elastoplastic Polycrystals, J. Mech. Phys. Solids **13**, 89-101 (1965).

[15] G. Sachs, On the Derivation of a Condition of Flow, Z. Verein. Deutsch. Ing. **72**, 739-747 (1928).

[16] I. Taylor, Plastic Strain of Metals, J. Inst. Met. **62**, 307-324 (1938).

[17] E. Kröner, Zur plastischen Verformung des Vielkristalls, Acta Met. **9**, 155-165 (1961).

[18] R.J. Asaro, Micromechanics of Crystals and Polycrystals, Adv. in Appl. Mech. **23**, 1-115 (1983).

[19] P. Franciosi, M. Berveiller, A. Zaoui, Latent Hardening in Copper and Aluminium Single Crystals, Acta Met. **28**, 273-283 (1980).

[20] M. Wróbel, PhD Thesis, Texture and structure development in rolled single crystals of copper (in polish), Akademia Górniczo-Hutnicza, Kraków, Poland (1988).

[21] H.J. Bunge, Texture Analysis in Materials Science, Butterworths, London (1982).

[22] K. Wierzbanowski, Computer Simulation Study of Texture Transitions in F.C.C. Metals and Alloys, Proc. of the 5-th Intern. Conf. on Textures of Materials, Ed. by G. Gottstein and Lücke **1**, 309-317, Springer Verlag, Berlin, Germany (1978).

[23] T. Leffers, R.K. Ray, The brass-type texture and its derivation from the copper-type texture, Progress in Materials Science **54**, 351-396 (2009).

[24] J. Tarasiuk, K. Wierzbanowski, Application of the Linear Regression Method for Comparison of Crystallographic Textures, Phil. Mag. A **73**, 1083-1091 (1996).

[25] K. Wierzbanowski, R. Wawszczak, A. Baczmański, J. Tarasiuk, Ph. Gerber, B. Bacroix and A. Lodini, Residual Stress and Stored Energy in Recrystallized Polycrystalline Copper, Archives of Metallurgy and Materials **50**, 201-207 (2005).

[26] K. Piękoś, J. Tarasiuk, K. Wierzbanowski, B. Bacroix, Recrystallization Study Using Two-Dimensional Vertex Model, Archives of Metallurgy and Materials **50**, 131-138 (2005).

[27] A. Baczmański, K. Wierzbanowski, J. Tarasiuk, M. Ceretti, A. Lodini, Anisotropy of Micro-Stress-Measured by Diffraction, Revue de Metallurgie **94**, 1467-1474 (1997).

[28] K. Wierzbanowski, J. Tarasiuk, B. Bacroix, A. Miroux, O. Castelnau, Deformation Characteristics Important for Nucleation Process. Case of Low-Carbon Steels, Archives of Metallurgy **44**, 183-201 (1999).

Received: 10 February 2011.